Scientia Iranica A (2011) 18 (3), 326–337

Sharif University of Technology

Scientia Iranica

Transactions A: Civil Engineering

www.sciencedirect.com

Application of the endurance time method in seismic analysis of concrete gravity dams

V. Valamanesh, H.E. Estekanchi *, A. Vafai, M. Ghaemian

Department of Civil Engineering, Sharif University of Technology, Tehran, P.O. Box 11155-9313, Iran

Received 5 July 2010; revised 19 March 2011; accepted 24 April 2011

KEYWORDS

Endurance time method;
Acceleration functions;
Concrete gravity dams;
Seismic analysis.

Abstract In this paper, application of the Endurance Time (ET) method in seismic analysis of concrete gravity dams has been investigated. The ET method is based on time history analysis of structures, subjected to specially designed intensifying acceleration functions. It is expected that by developing its application in analysis of concrete dams, useful information on the seismic behavior of such dams at various excitation intensities can be obtained. Results from linear analysis of Folsom and Koyna dams under real earthquakes and ET acceleration functions have been compared. It is shown that the ET method can predict the response of concrete gravity dams to individual earthquakes with reasonable accuracy in linear analysis. In order to evaluate concrete gravity dams by linear analysis, the target time has been assumed to correspond to the OBE level of earthquake. Endurance criteria can be set as the time when the desired damage index(es), e.g. maximum principal stress, reaches its allowable value. The design can be considered satisfactory if endurance time is more than target time and vice versa. Also, potential application of the ET method in non-linear analysis of concrete gravity dams has been investigated. It is shown that crack profiles during earthquakes could be traced by the ET method.

1. Introduction

The basic objective of seismic design is to provide structures with appropriate safety margins against failure when subjected to strong earthquakes. Concrete dams are among high importance structures, regarding requirements for continuous service during their lifetime, and catastrophic effects in cases of probable dam failure. Therefore, the safety of these structures should be investigated quite critically by logical and precise methods.

With the improvement of knowledge in earthquake engineering and the development of more reliable methods for estimating earthquake magnitudes at different sites, methods for the seismic analysis of structures are being developed that include the effects of more complicated parameters in the evaluation and seismic hazard analysis of structures.

* Corresponding author.
E-mail address: stkanchi@sharif.edu (H.E. Estekanchi).

1026-3098 © 2011 Sharif University of Technology. Production and hosting by Elsevier B.V. Open access under CC BY-NC-ND license.
Peer review under responsibility of Sharif University of Technology.

doi:10.1016/j.scient.2011.05.039

Production and hosting by Elsevier

In the Endurance Time procedure, structures are subjected to a set of specially designed intensifying accelerograms, the response spectra of which increase proportionally with time, and the Endurance Time of the structures are measured based on the time interval during which they can resist the imposed dynamic excitations.

In this paper, using the ET method and considering the elastic analysis procedure, the dynamic performance of two well known concrete dams under Operation Based Earthquake (OBE) are evaluated. The basics of the ET procedure are briefly reviewed. The results of the Endurance Time analyses of Folsom and Koyna dams, taking into account dam-reservoir interaction under ET acceleration functions, have been presented and compared to an equivalent response spectrum analysis and also time history analysis, under real earthquakes.

In non-linear analysis, using the smeared crack approach, the performance of the Koyna dam under ET acceleration functions is investigated and the potential of the ET method in non-linear analysis of concrete dams is evaluated. It is shown that the seismic behavior of concrete gravity dams can be predicted by the ET method with reasonable approximation.

2. Endurance time concept

The Endurance Time method has been introduced [1] as a new seismic analysis method and, in further investigations, application of this method in the linear analysis of steel frames

was assessed [2]. Also, application of this method in nonlinear seismic analysis of steel frames has been investigated [3,4], and application of the ET method in linear analysis of concrete gravity dams has been investigated by the authors [5]. In the ET method, structures are subjected to a set of specially designed intensifying accelerograms, called "ET acceleration functions", in a manner wherein the response spectra of such acceleration functions linearly increase by time, and whose seismic performance is judged based on the time interval during which they can endure the imposed dynamic excitation.

In ET analysis, endurance time is considered to be the time when the maximum value of the specified design parameter, such as drift or stress, exceeds the maximum allowable value. For convenience, design parameters are usually normalized based on their maximum allowable values, i.e. endurance time is defined as the time when the ratio of the response parameter (such as drift or stress) to its allowable value exceeds one. In order to decide whether or not the achieved endurance time can be considered adequate, the intensity of the imposed dynamic action at this time should be considered. Spectral acceleration is the most popular intensity measure used in practice and has been considered for calibrating the ET acceleration functions used in this study.

2.1. Characteristics of ET acceleration functions

As shown later, particular ET acceleration functions considered in this study have been calibrated in such a way that not only do their response spectra match that of the template code spectra at $t = 10$ s, but also at all other times, the shape of the response spectra remains proportional to the template spectra. The time at which the response spectrum of an ET acceleration function matches the template response spectra with a scale factor of unity is called the *target time*. According to this definition, the target time of ET acceleration functions in this study is set to $t = 10$ s.

Another characteristic of ET acceleration functions is that they linearly intensify by time. In this way, if the window of an acceleration function is taken from $t = 0$ s to $t = 5$ s, its response spectrum corresponds to half of the template spectra at all periods. If the interval of $t = 0$ s to $t = 15$ s is taken, its response spectrum matches 1.5 times the template spectrum. Therefore, for a certain structure designed according to the template spectrum, if, for example, the drift ratio exceeds its limit at $t = 15$ s, it can be concluded that the structure satisfies the drift criteria, since its endurance time is more that required by the code, i.e. a minimum endurance time of 10 s in this case.

A schematic ET analysis result for three hypothetical frames (or, say, three different designs for the same frame), under an ET acceleration function (Figure 1) has been depicted in Figure 2. If a limiting Demand/Capacity parameter (such as the ratio of drift or stress to their allowable values) is considered, the behavior of these structures can be compared considering these ET curves. As seen in Figure 2, Frame 2 turns out to be the best performer, while Frame 1 is the worst performer in this analysis. Details of application of the ET method have been explained in related literature [6].

It should be noted that an ET analysis result includes an estimate of the response under different levels of excitation in each single analysis. In this way, an approximate overall image of structure response can be generated by a limited number of time–history analyses.

2.2. Calibration of second generation of ET acceleration functions

The first generation of ET acceleration functions was based on peak acceleration [1], while in the second generation of ET

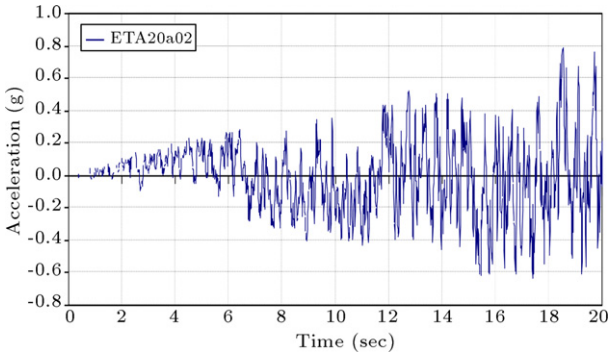

Figure 1: An ET acceleration function (ETA20a02).

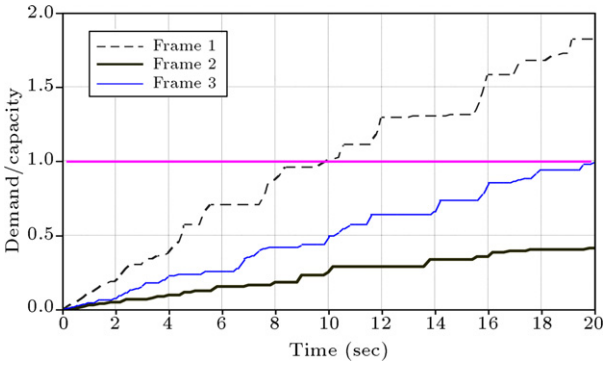

Figure 2: Demand/capacity of frames under ET acceleration functions action.

acceleration functions, the concept of a response spectrum is more directly involved. By scaling the ET acceleration functions using a simple linear scale factor, Sa (and Sd) can be set to reach the required target level at any desired time. In this way, we define the target response of ET acceleration functions as in Eqs. (1) and (2):

$$S_{aT}(T, t) = \frac{t}{t_{Target}} S_{aC}(T), \tag{1}$$

$$S_{uT}(T, t) = \frac{t}{t_{Target}} S_{aC}(T) \times \frac{T^2}{4\pi^2}, \tag{2}$$

where $S_{aT}(T, t)$ is the target acceleration response at time t, T is the period of free vibration, $S_{aC}(T)$ is the codified design acceleration spectrum, and $S_{uT}(T, t)$ is the target displacement response at time t. The problem of generating an accelerogram with such characteristics was approached by formulating it as an unconstrained optimization problem in the time domain as follows:

$$\text{Minimize } F(a_g) = \int_0^{T_{\max}} \int_0^{t_{\max}} \{[S_a(T, t) - S_{aT}(T, t)]^2 + \alpha[S_u(T, t) - S_{uT}(T, t)]^2\} \mathrm{d}t \, \mathrm{d}T, \tag{3}$$

where a_g is the ET accelerogram being sought and α is an optimization weighting parameter, set to 1.0 in this study. In order to proceed with numerical calculations, a typical code compliant accelerogram that corresponds to standard No. 2800 of the Iranian National Building Code (INBC) has been used to define the target response. As a sample, an ET acceleration function (ETA20a02) produced by this procedure has been depicted in Figure 1. Acceleration response spectra of the first set of three ET acceleration functions (i.e. ETA20a01, ETA20a02

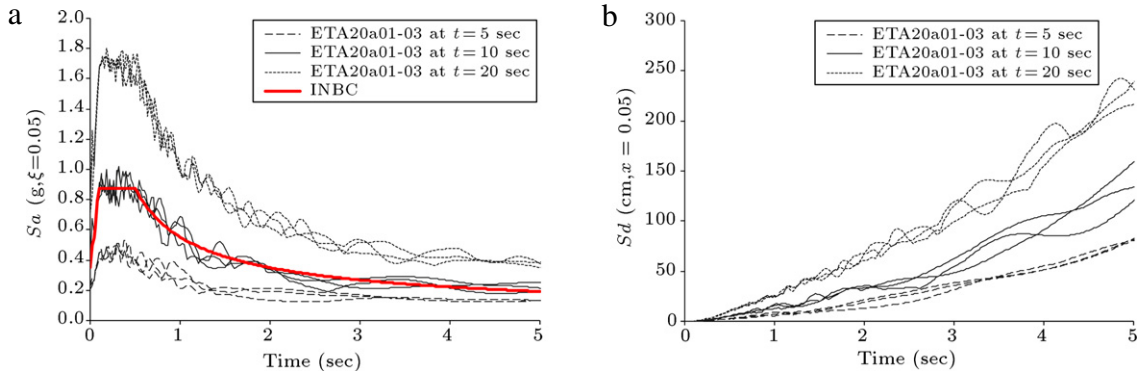

Figure 3: Response spectra of ETA20a series accelerograms for $\xi = 5\%$ at different times. (a) Pseudo-acceleration; (b) displacement response.

and ETA20a03) at $t = 5$ s, $t = 10$ s and $t = 20$ s are depicted in Figure 3a. The target time for this set of ET acceleration functions has been set to 10 s; therefore, the response at $t = 10$ s should match the codified value with a scale factor of unity. At $t = 5$ s and $t = 20$ s, the response spectra of ET acceleration functions should match one-half and twice the standard codified values, respectively. Displacement responses of these acceleration functions at various times are depicted in Figure 3b. As expected, displacements follow the target values defined by Eq. (2), with almost the same level of dispersion as the acceleration responses. As seen in Figure 3, the optimization process has been quite successful in converging to the target values.

2.3. Compatibility of ET method in linear seismic analysis

As the OBE level of earthquakes is defined in terms of PGA or the response spectrum curve, in the ET method, a specific time should be defined in such a way that it can be representative of the OBE level. On the other hand, occurred damage at that time should be equal to damage under earthquakes with the same OBE level. For this purpose, the concept of equivalent time is defined as follows.

By using the SRSS modal combination, base shear, maximum displacement and acceleration of response are achieved as follows:

$$Q_{\max} = \sqrt{\sum_{i=1}^{n} Q_i^2} = \sqrt{\sum_{i=1}^{n} \left(\frac{L_i^2}{M_i}.(Sa_i)\right)^2}, \tag{4}$$

$$y_{\max} = \sqrt{\sum_{i=1}^{n} y_i^2} = \sqrt{\sum_{i=1}^{n} \left(\frac{L_i}{M_i}.(Sd_i)\right)^2} = \sqrt{\sum_{i=1}^{n} \left(\frac{L_i}{M_i.\omega_i^2}.(Sa_i)\right)^2}, \tag{5}$$

$$\ddot{y}_{\max} = \sqrt{\sum_{i=1}^{n} \ddot{y}_i^2} = \sqrt{\sum_{i=1}^{n} \left(\frac{L_i}{M_i}.(Sa_i)\right)^2}, \tag{6}$$

where $\frac{L_i}{M_i}$ is the Modal participation factor and $Q, y, \ddot{y}$ are base shear, displacement and acceleration, respectively. If the standard spectrum in the ith mode is Sa_i^s and the design response spectrum in the ith mode with natural frequency, ω_i, is Sa_i^R, the ratio of the response spectrum in each mode can be obtained from Eq. (7):

$$R_i = \frac{Sa_i^R}{Sa_i^s}. \tag{7}$$

Ignoring statistical dispersions, the response spectrum of ET acceleration functions at $t = 10$ s is equal to the standard spectrum with $A = 0.35$ g, according to the INBC No. 2800 code. Therefore, Eq. (7) can be used as the ratio of the design response spectra and the response of ET acceleration functions at $t = 10$ s in each mode. Knowing that the response spectra of acceleration functions are linearly proportional with time, based on the desired response index, the equivalent time in the ET method can be computed as follows:

$$t_e^Q = 10 \times \frac{Q_{\max}^R}{Q_{\max}^s} = \sqrt{\frac{\sum_{i=1}^{n} Q_i^{R2}}{\sum_{i=1}^{n} Q_i^{s2}}} = \sqrt{\frac{\sum_{i=1}^{n} \left(\frac{L_i^2}{M_i}.(R_i.Sa_i^s)\right)^2}{\sum_{i=1}^{n} \left(\frac{L_i^2}{M_i}.(Sa_i^s)\right)^2}}, \tag{8}$$

$$t_e^{\ddot{y}} = 10 \times \frac{\ddot{y}_{\max}^R}{\ddot{y}_{\max}^s} = \sqrt{\frac{\sum_{i=1}^{n} \ddot{y}_i^{R2}}{\sum_{i=1}^{n} \ddot{y}_i^{s2}}} = \sqrt{\frac{\sum_{i=1}^{n} \left(\frac{L_i}{M_i}.(R_i.Sa_i^s)\right)^2}{\sum_{i=1}^{n} \left(\frac{L_i}{M_i}.(Sa_i^s)\right)^2}}, \tag{9}$$

$$t_e^y = 10 \times \frac{y_{\max}^R}{y_{\max}^s} = \sqrt{\frac{\sum_{i=1}^{n} y_i^{R2}}{\sum_{i=1}^{n} y_i^{s2}}} = \sqrt{\frac{\sum_{i=1}^{n} \left(\frac{L_i}{M_i.\omega_i^2}.(R_i.Sa_i^s)\right)^2}{\sum_{i=1}^{n} \left(\frac{L_i}{M_i.\omega_i^2}.(Sa_i^s)\right)^2}}, \tag{10}$$

in which $t_e^Q, t_e^{\ddot{y}}, t_e^y$ are equivalent times based on base shear, acceleration and displacement response, respectively.

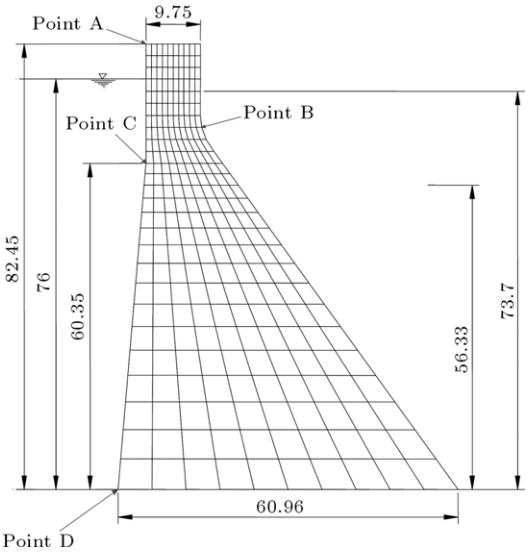

Figure 4: Geometric properties and finite element model of Folsom dam.

In summary, it is expected that the linear response of concrete dams in the equivalent time of an earthquake or design spectrum should be equal to the maximum response of a dam under a real earthquake or design spectrum. In the following sections, it is explained in more detail.

3. Models of concrete dams and real earthquakes

Two concrete gravity dams, i.e. Koyna and Folsom, are used in this study. These dams were studied by many researchers, so the results can be verified with already published material. In linear analysis, the Westergaard method is used in order to include dam-reservoir interaction.

In this paper, the ETA20a series of ET acceleration functions, which are calibrated based on the standard response spectrum for soil type 2, according to the Iranian National Building Code (INBC standard 2800), are used for seismic analysis of concrete gravity dams using the ET method.

3.1. Folsom dam

The Folsom dam has been constructed on an American river, about 32 km northeast of the city of Sacramento. The dam section consists of 28 monoliths, each of which is 15.2 m wide. The tallest section is 82.45 m high and 60.96 m wide at the base. In Figure 4, geometric properties and the finite element model of the dam are shown. This dam was studied earlier by researchers [7]. In this analysis, dam-foundation interaction is omitted and, assuming incompressibility of the fluid, the generalized Westergaard method is used for dam-reservoir interaction. A 5% linear viscous damping is considered using proportional damping for the first mode of vibration. The modulus of elasticity of the concrete is 40679 MPa, and the Poisson ratio and tensile strength of the concrete are assumed to be 0.19 and 3.2 MPa (including a 1.2 dynamic magnification factor), respectively [8].

The modal properties of the dam, including dam-reservoir interaction, for the first 5 modes, are shown in Table 1.

To compare results of the ET method with time history analysis under real earthquakes, four real accelerograms, which are scaled to PGA = 0.3 g, are used. These accelerograms are listed in Table 2, and their response spectra are illustrated and compared with the standard response spectrum for soil condition type 2, according to the INBC code (Figure 5).

Table 1: Modal properties of Folsom dam with dam-reservoir interaction.

Mode	Period	Frequency, Hz	Mass X	Sum mass X
1	0.2218	4.51	0.400	0.40
2	0.0996	10.04	0.280	0.68
3	0.0591	16.92	0.077	0.76
4	0.0549	18.21	0.0846	0.85
5	0.0374	26.71	0.0556	0.90

Table 2: Real accelerograms used for elastic analysis of Folsom dam.

Accelerogram	Station	Scaled PGA
1996 Park Field	Cholame #8	0.3 g
1989 Loma Prieta	Gavilan college	0.3 g
1987 Whittier Narrows	Garvey reservoir	0.3 g
1971 San Fernando	Pacoima dam	0.3 g

Table 3: Comparison of equivalent time according to various indexes.

Parameter	Park Field	Loma Prieta	Whittier Narrows	San Fernando	Avr-EQs
t_e^Q	9.37	9.2	8.9	5.95	8.33
$t_e^{\dot{y}}$	8.73	8.72	8.7	6.07	8.3
t_e^y	10.63	9.82	8.8	5.77	8.75
1st mode	10.74	9.87	8.79	5.76	8.8

It is evident that due to modal periods and their importance in the response of the structure, results of the time history analysis under real earthquakes can be equal to or different from the response spectrum analysis. In this case, it seems that the response spectra of earthquakes are not similar to the standard response spectrum during moderate and long periods. However, the average of these response spectra, during short periods, which is expected for concrete gravity dams, is near to the standard spectrum.

Having modal specifications of dams and response spectra of earthquakes, the equivalent time can be derived, as they are compared with the equivalent time, based on the first mode of vibration (Table 3).

According to structural codes, base shear is a design criterion, and accelerograms are scaled in such a way that the base shears from individual records are the same. Using a similar concept, the average equivalent time of these four accelerograms, with PGA = 0.3 g, could be taken as $t = 8.33$ s.

3.2. Koyna dam

The Koyna dam in India suffered very serious damage during the Koyna earthquake in 1967. The first linear analysis was carried out in 1972 [9]. The tallest section of this dam is shown in Figure 6. For linear analysis, stiffness proportional damping, equivalent to 5% damping, is used. The modulus of elasticity and the Poisson ratio of the concrete are taken as 30,000 MPa and 0.2, respectively. The tensile and compressive strength of the concrete are taken to be 2.9 and 24.1 MPa, respectively. And a dynamic magnification factor of 1.2 is considered for the tensile strength.

Modal properties of the Koyna dam, taking into account dam-reservoir interaction, are listed in Table 4. Horizontal and vertical components of the Koyna earthquake are

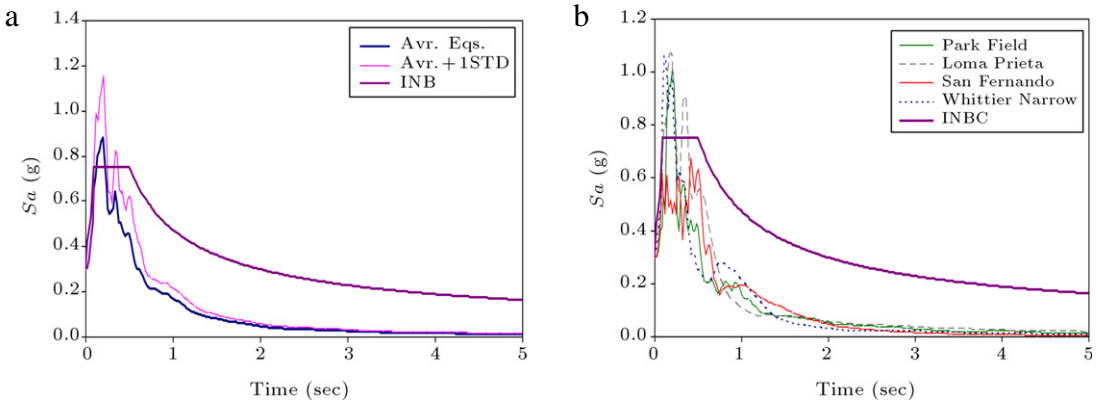

Figure 5: Comparison of response spectra of scaled real earthquakes with INBC standard response spectrum for soil condition type 2 with PGA = 0.3 g.

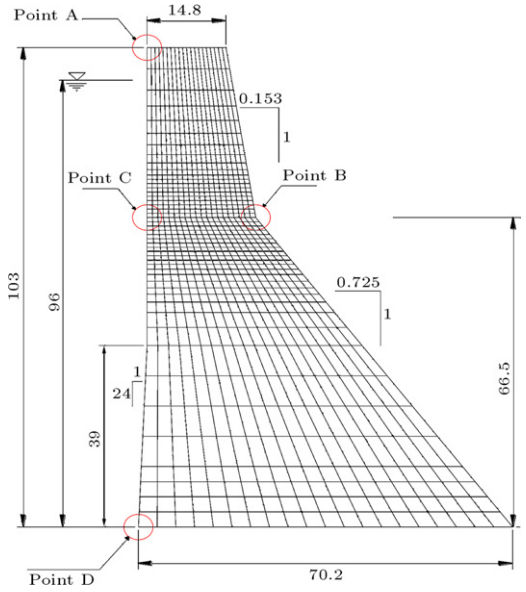

Figure 6: Koyna dam specifications.

Table 4: Modal properties of Koyna dam including dam-reservoir interaction.

Mode	Period	Frequency, Hz	Mass X	Sum mass X
1	0.387	2.58	0.378	0.378
2	0.149	6.69	0.292	0.669
3	0.093	10.68	0.051	0.72
4	0.078	13.73	0.112	0.832
5	0.053	18.07	0.049	0.88
6	0.042	23.70	0.016	0.896
7	0.042	24.06	0.00387	0.90
8	0.037	27.17	0.015	0.915

shown in Figure 7 and their response spectra are compared to the standard spectrum, according to the INBC code (Figure 8).

Considering base shear, the equivalent time for horizontal and vertical components of the Koyna earthquakes will be 8.52 s and 7.74 s, respectively.

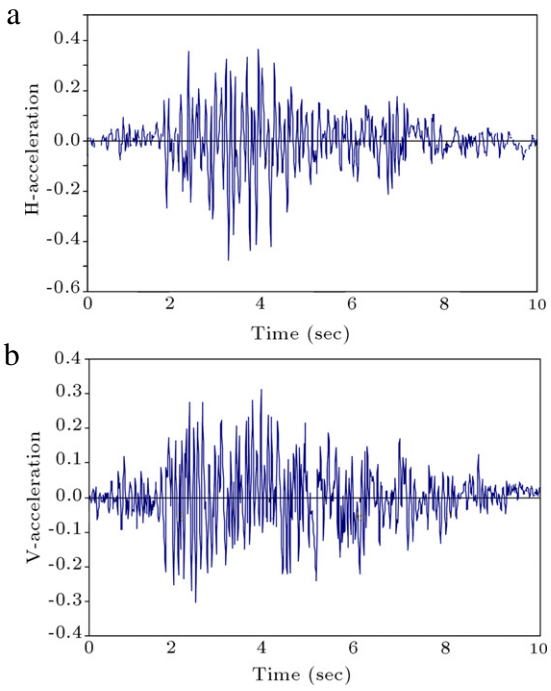

Figure 7: Koyna accelerograms. (a) Horizontal Acc.; and (b) vertical Acc.

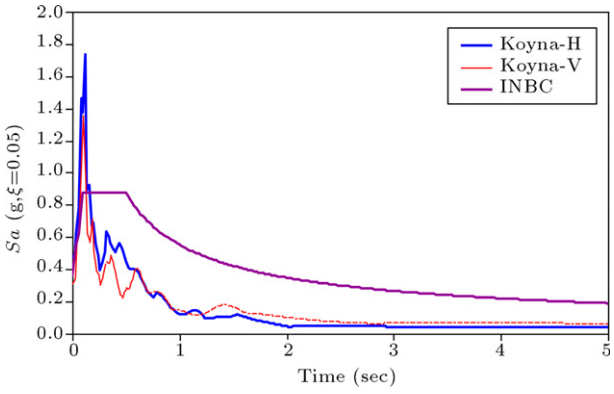

Figure 8: Comparison of response spectra of Koyna earthquake and standard spectrum.

4. Linear analysis of concrete gravity dams

According to USACE guidelines in linear analysis three major indexes have been studied, i.e. displacement at the crest of the dam, tensile stress and cumulative inelastic duration.

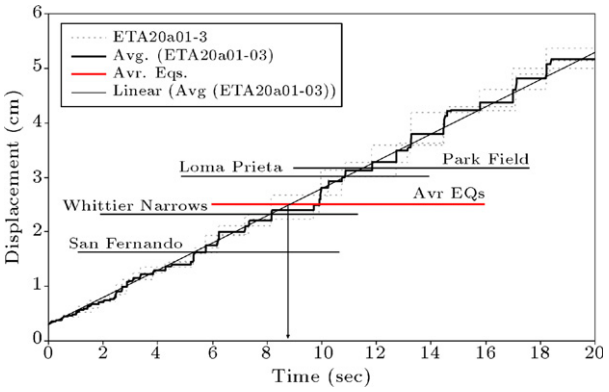

Figure 9: Displacement at crest of Folsom dam.

Table 5: Comparison of maximum displacement (cm) regarding direction of excitations.

	Park Field	Loma Prieta	Whittier Narrows	San Fernando	Avr-ETA01-03
DL + HL + EQ	3.01	2.45	1.55	2.26	2.61
DL + HL − EQ	2.55	2.9	1.44	2.21	2.605
Difference%	15.3	15.51	7.1	2.2	0.4

4.1. Folsom dam

4.1.1. Displacement

Considering initial displacement due to hydrostatic pressure, results of displacement for the four mentioned earthquakes and ET acceleration functions are depicted in Figure 9.

As seen, displacement at the crest reaches the value of Park Field, Loma Prieta, Whittier Narrows and San Fernando earthquakes at $t = 11$ s, 10.6 s, 8.1 s and 5.5 s, respectively. Comparing these times with equivalent time of displacement from Table 3, the differences are calculated as 3.3%, 7.9%, 7% and 4.7%, and the average difference is 5.7%.

Also, it is obvious that at around the equivalent time, i.e. $t = 8.33$ s, maximum displacement of the dam coincides with the average of displacement from four real earthquakes, which are scaled to PGA $= 0.3$ g. An important aspect of ET acceleration functions is simplicity in combination with other loads. In Table 5, a comparison between results of displacement, due to accelerograms in two opposite directions, shows that displacement in the dam is not sensitive to the direction of ET acceleration functions.

4.1.2. Tensile stress

Comparison of tensile stress at critical points (i.e. B, C and D in Figure 6) from real earthquakes and ET acceleration functions are illustrated in Figure 10, and prediction of the strength of critical points by ET acceleration functions is illustrated in Figure 11.

As seen in Figure 10, the ET method gives the same results from the average of real earthquakes at time 8–10 s, as expected by the equivalent time derived previously. The average difference is 8% and the maximum difference is below 18%, in this case.

From Figure 11, it can be concluded that at $t = 5.2$ s, the tensile stress at point B exceeds its allowable value. Related PGA for $t = 5.2$ s is $\frac{5.2}{10} \times 0.35 = 0.182$ g (see Eq. (1)).

A study of load combinations and stresses provides information about the effects of seismic loading in two opposite directions. In Table 6, results of maximum tensile stress at critical points, due to two opposite direction excitations, under real earthquakes and ET acceleration functions, are shown.

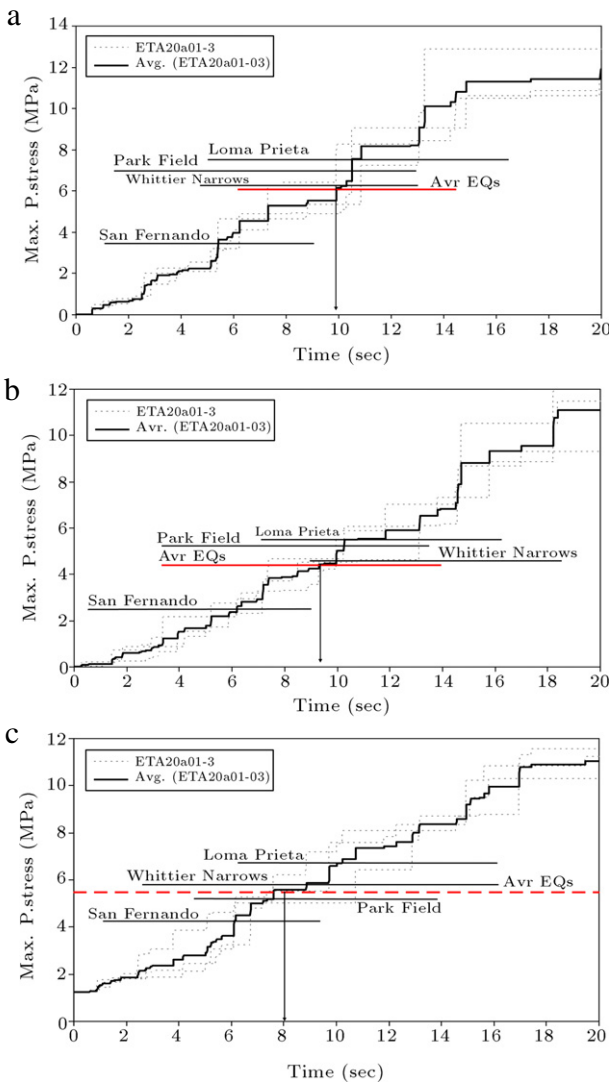

Figure 10: Maximum tensile stress in critical points under real earthquakes and ET acceleration functions, (a) point B; (b) point C; and (c) point D.

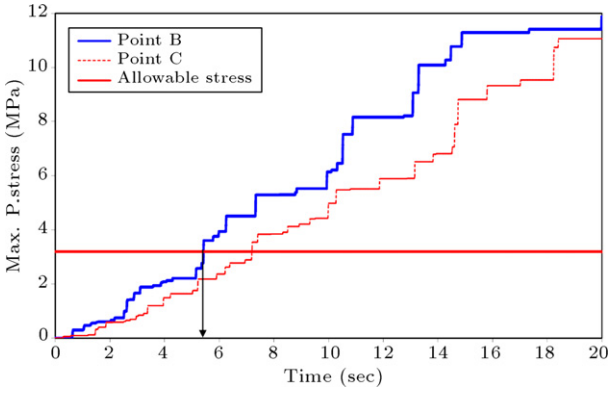

Figure 11: Evaluation of stress with ET acceleration functions.

Table 6: Comparison of maximum tensile stress (MPa) regarding direction of earthquake excitation.

Point	Load Comb.	Park Field	Loma Prieta	Whittier Narrows	San Fernando	Avr-ETA01-03
B	DL + HL + EQ	5.24	7.51	3.37	5.18	6.6
	DL + HL − EQ	7.05	4.45	3.18	6.32	6.592
C	DL + HL + EQ	5.1	3.165	2.21	4.55	5.17
	DL + HL − EQ	3.81	5.41	2.43	3.64	4.82
D	DL + HL + EQ	5.16	6.65	4.18	4.73	6.39
	DL + HL − EQ	5.25	4.98	4.16	5.73	6.4
	Difference%	17.5	35.7	5.0	18.4	2.3

Note that stresses at point D (base) of the FE model cannot be reliable, due to stress concentration in this location, and have been included just for the purpose of comparison. The average difference between two opposite loadings, for ET acceleration functions, is 2.3%, while this value for other earthquakes can be high. In this regard, it can be concluded that it is not necessary to apply ET acceleration functions in two opposite directions, while it is required for biased real earthquakes.

4.2. Koyna dam

4.2.1. Displacement

Displacement responses of the Koyna dam under different earthquake load combinations are shown in Table 7. These analyses include the effect of a vertical earthquake combination, as well as hydrodynamic effects.

To perform analyses of the dam, considering the vertical ET acceleration function, the ET acceleration functions are scaled in such a way that the ratio between vertical and horizontal components of the Koyna earthquake is simulated. Therefore, each ET acceleration function, as a vertical component, is scaled by the ratio of vertical and horizontal equivalent times, i.e. $F_{Sc} = \frac{t_{eq}^{V}}{t_{eq}^{H}} = \frac{7.74}{8.52} = 0.908$. Displacements of the Koyna dam, in two states of horizontal and a combination of horizontal and vertical accelerations, are compared with Koyna earthquakes in Figure 12. In these figures, H and V represent horizontal and vertical displacements at the top of the Koyna dam, respectively.

It is evident from these figures that maximum displacement at $t = 8.5$ s reaches the value of the Koyna earthquake. Also, the vertical component increases displacement for both ET acceleration functions and the Koyna earthquake, but has no important effect on differences between ET and Koyna accelerograms. Also, at the same time of $t = 8.5$ s, displacements from the ET method reach the value of the Koyna earthquake.

4.2.2. Tensile stress

Investigations have shown that three points, B, C and D, are susceptible to be cracked [9]. Therefore, in Figure 13, for these three points, the principal stress is sketched for the Koyna earthquake. It is evident that these points are weak under the Koyna earthquake, as their stresses go beyond the limit at the beginning of analyses. This observation is confirmed by the ET method, as tensile stress at points B, C and D reach their allowable stress just at the beginning of analyses, i.e. 3, 5.5 and 2 s, respectively (Figures 14 and 15), while the equivalent time of the Koyna earthquake is about 8.5 s. Also, it can be seen that at the equivalent time, maximum tensile stress is equal to the results of the Koyna earthquake. Again, note that stresses at point D (base) of the FE model cannot be reliable, due to stress concentration in this location and have been included just for purposes of comparison.

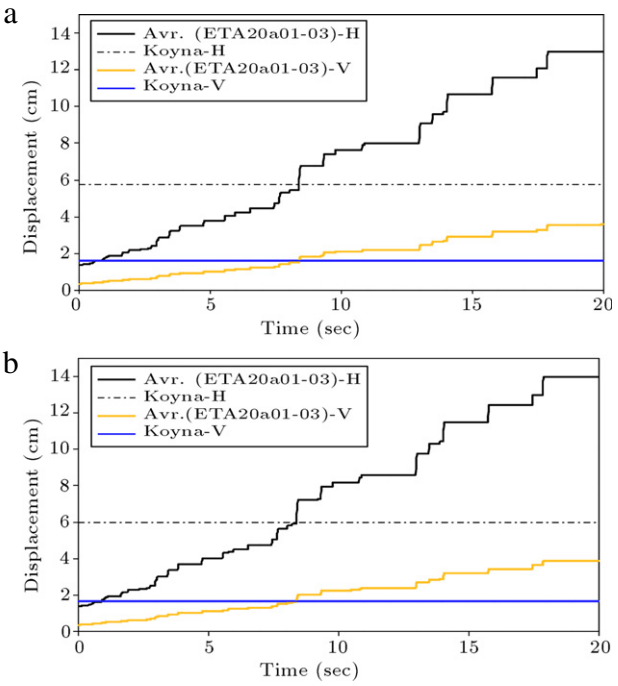

Figure 12: Maximum displacement of dam. (a) Horizontal Acc.; and (b) horizontal and vertical Acc.

It is apparent that endurance time according to tensile stress in linear analyses is around 2 s, i.e. tensile stress in the Koyna dam, under ET acceleration functions, reaches its allowable stress within 2 s from the beginning of analysis. Related PGA is $\frac{2}{10} \times 0.35$ g $= 0.07$ g. This value seems to be very low for the seismic strength of dams, which confirms that the Koyna dam is vulnerable to moderate and strong ground motions. In this manner, it can be seen how the ET method can predict the weakness of a dam during such earthquakes.

Further investigation reveals that stress distributions in the Koyna dam under the Koyna earthquake is equal to that from ET acceleration functions at $t = 8.5$ s.

In the above discussion, we have seen that based on linear analysis, at an equivalent time, i.e. $t = 8.5$ s, the same results from the Koyna earthquake and ET acceleration functions will be obtained, but one knows that after crack initiation in concrete dams, linear analysis will not be reliable and nonlinear analysis is necessary to get more accurate results. A quantitative limit has been introduced [10], which is shown for the Koyna dam in Figure 16, under the Koyna earthquake, and at different times (i.e. $t = 2, 3, 5, 7, 9$ s) for the average of ET acceleration functions.

Table 7: Maximum earthquake response of Koyna dam.

Static load	H-Acc.	V-Acc.	Acceleration (m/s^2)		Velocity (cm/s)		Displacement (cm)	
			Horizontal	Vertical	Horizontal	Vertical	Horizontal	Vertical
+	+	0	−29	−12.8	−90	−29.2	5.723	1.57
+	−	0	29	12.8	90	29.2	4.447	1.32
+	+	+	−30	22.2	−87.4	34.8	5.48	1.527
+	+	−	−28.7	24.4	−93.2	−39	5.943	1.64
+	−	+	28.7	−24.4	93.2	39	4.77	1.59
+	−	−	30	−22.2	87.4	−34.8	4.4	1.26

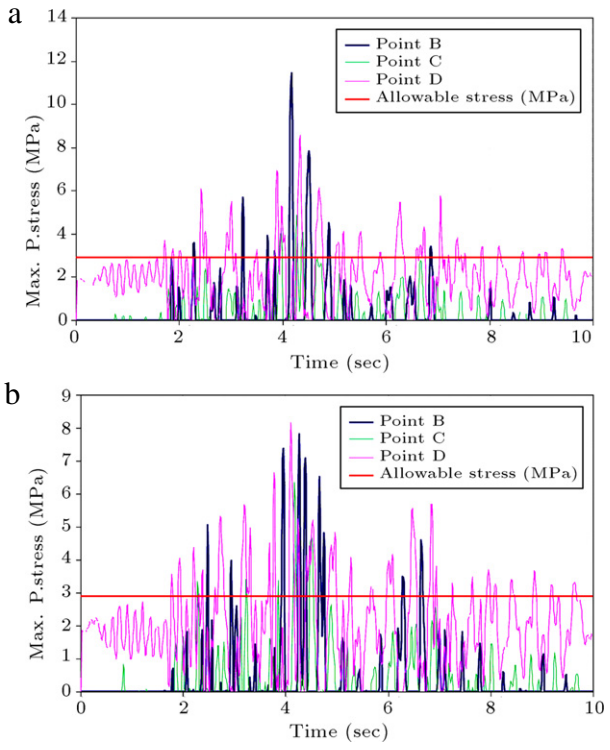

Figure 13: Maximum principal stress under Koyna earthquake. (a) Horizontal Acc.; and (b) horizontal and vertical Acc.

Using this criteria, nonlinear analysis is necessary for both the Koyna earthquake and also ET acceleration functions after $t = 5$ s. As will be shown later, using the displacement response of the Koyna dam by the ET method, this conclusion could be achieved.

5. Endurance time approach for linear seismic analysis

As mentioned, using the ET method and based on tensile stress in the Koyna dam, related PGA for the OBE level is 0.07 g; this value will be higher if point D is omitted (the stress at point D is not reliable because of stress concentration). To evaluate this PGA using a compatible earthquake, we use 7 real earthquakes recorded in soil type C, according to NEHRP provisions, which are similar to soil condition type 2 in the INBC code. These accelerograms are listed in Table 8.

Response spectra of these accelerograms, which are scaled to PGA = 0.35 g, are compared to ET acceleration functions and also the standard response spectrum, according to the INBC code (Figure 17).

Although there is a large difference between each real earthquake and ET acceleration functions, the average response

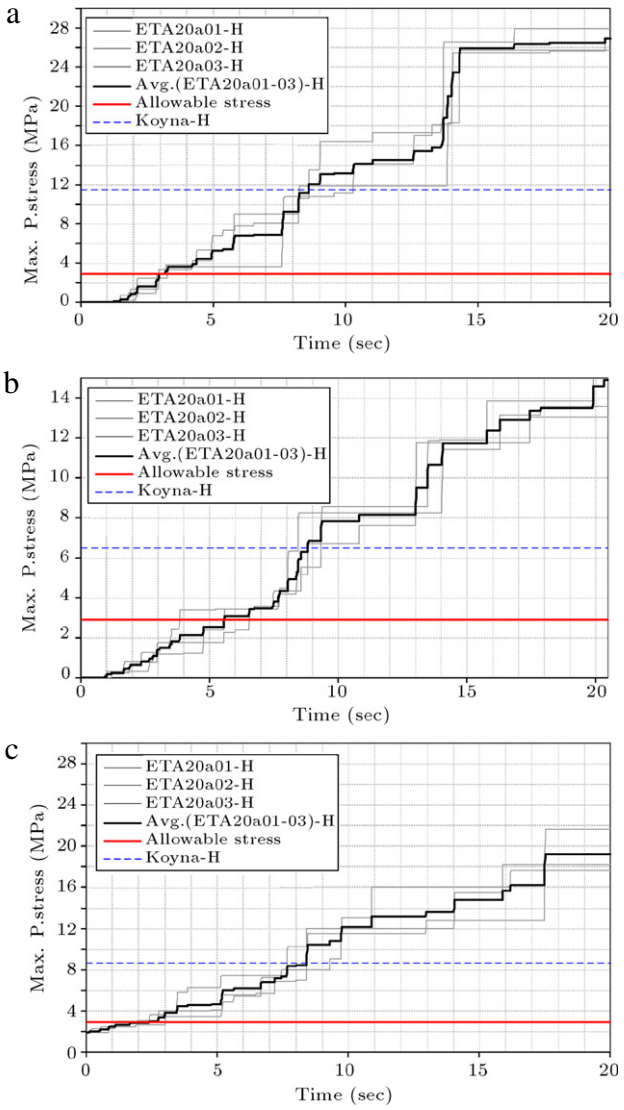

Figure 14: Comparison of stress for ET acceleration functions and Koyna horizontal accelerograms. (a) point B; (b) point C; and (c) point D.

spectra of these earthquakes is nearly compatible with the standard response spectrum during short periods, i.e. $T < 0.5$ s, which includes the range of most common concrete gravity dams. At first, these accelerograms are scaled to PGA = 0.07 g, which was derived by the ET method, then the Koyna dam is analyzed by these accelerograms. The results of displacement and tensile stress from the average of these earthquakes are illustrated in Figure 18.

Table 8: Real earthquakes in soil type C according to NEHRP provisions.

Date	Name	EQ name	Magnitude	Station number	Component (deg)	PGA (cm/s^2)
06/28/92	LADSP000	Landers	7.5	12149	0	167.8
10/17/89	LPSTG000	Loma Prieta	7.1	58065	0	494.5
10/17/89	LPGIL067	Loma Prieta	7.1	47006	67	349.1
10/17/89	LPLOB000	Loma Prieta	7.1	58135	360	433.1
10/17/89	LPAND270	Loma Prieta	7.1	1652	270	239.4
04/24/84	MHG06090	Morgan Hill	6.1	57383	90	280.4
01/17/94	NRORR360	Northridge	6.8	24278	360	504.2

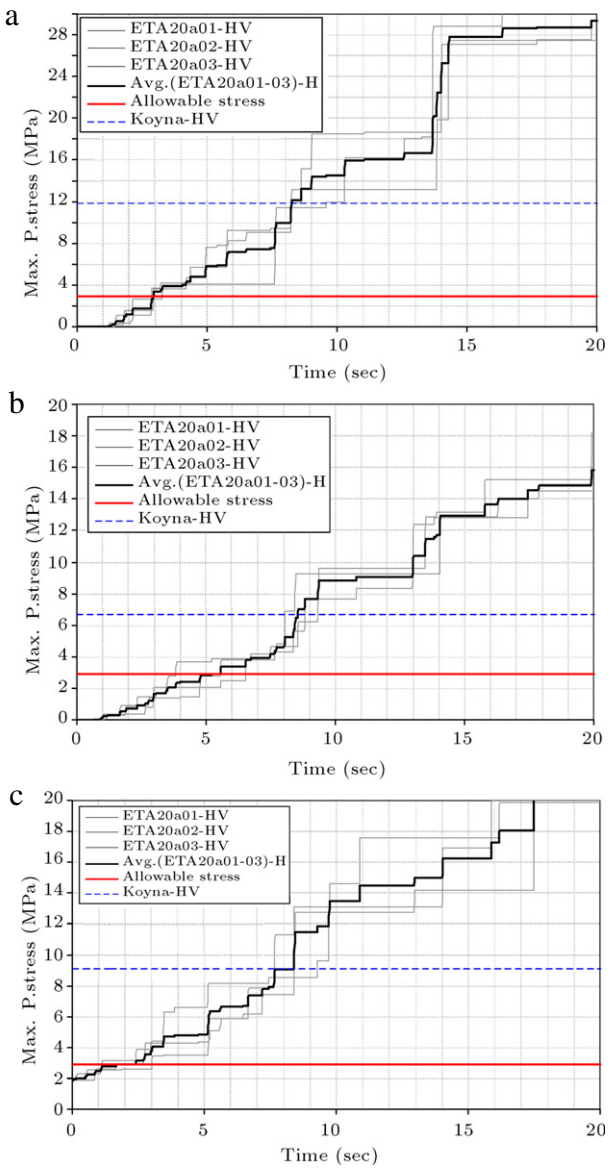

Figure 15: Comparison of stress for ET acceleration functions and Koyna horizontal and vertical accelerograms. (a) point B; (b) point C; and (c) point D.

From these figures, the difference in the results for the average of the earthquake and ET acceleration functions is below 20%. This difference can be acceptable, because the average response spectrum of these earthquakes is not exactly the same as the standard spectrum. It can be concluded that the ET method is very effective in the prediction of dam behavior in linear analysis under weak and moderate ground motion. For strong ground motion, a non-linear analysis is required, which is discussed in the following section.

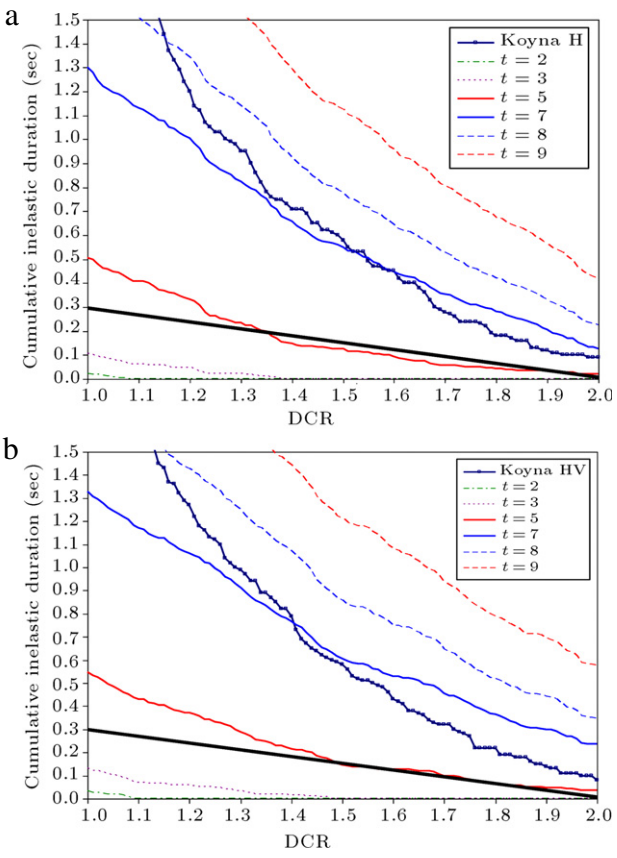

Figure 16: Cumulative Inelastic Duration (CID) via Demand Capacity Ratio (DCR) of Koyna dam. (a) Horizontal Acc.; and (b) horizontal and vertical Acc.

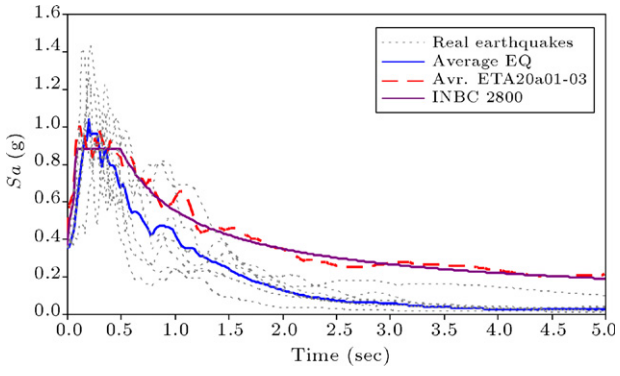

Figure 17: Comparison of response spectra of compatible real earthquakes, ET acceleration functions and INBC code.

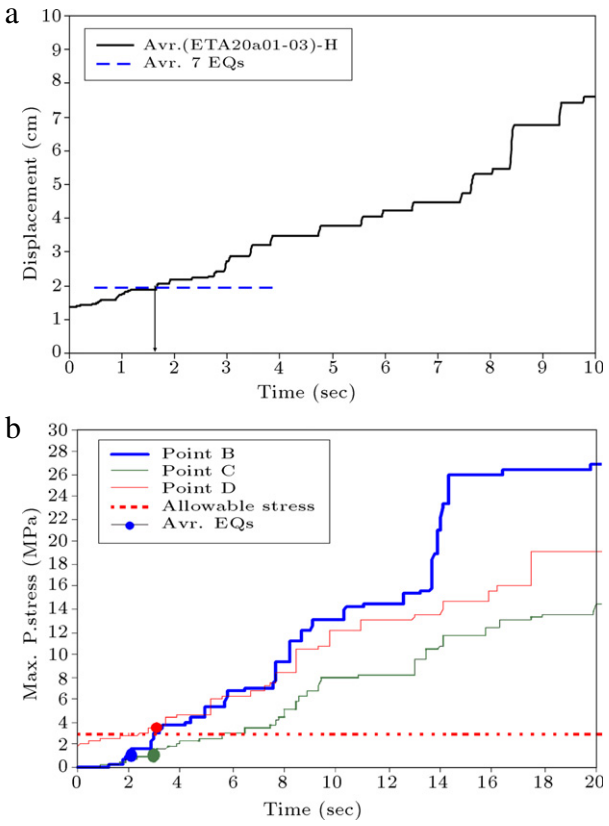

Figure 18: Comparison of displacement and tensile stress between average of earthquakes and ET acceleration functions. (a) Displacement; and (b) tensile stress.

6. Non-linear analysis

In the analysis of the Koyna dam, damage grows in such a way that a linear procedure cannot be considered reliable. Therefore, a nonlinear approach is to be used. In a non-linear analysis procedure, modal combination is not applicable. Therefore, an advanced method for modeling of the structure, dam-reservoir interaction and crack initiation should be applied.

Most researchers have used three approaches to predict and trace crack propagation in concrete dams. Discrete crack [11], damage mechanic [12] and smeared crack [13] approaches have been proposed to model concrete behavior in the seismic analysis of concrete gravity dams. Ghaemian and Ghobarah [14] proposed a staggered solution for dam-reservoir interaction. In this section, non-linear analysis of the Koyna dam, due to the Koyna earthquake and ET acceleration functions, is conducted using a staggered displacement method for dam-reservoir interaction.

The smeared crack model, based on nonlinear fracture mechanics, is used to study the nonlinear behavior of concrete gravity dams [15]. The main features of the model are: (1) the strain softening of concrete due to micro cracking is included; (2) the fracture band is rotated with the progress of damage; (3) conservation of fracture energy is satisfied, and (4) the opening and closing of cracks under cycling loading conditions are represented.

In 2003, Asteris and Tzamtzis used the finite element method and especially developed elements to propose a new methodology for the response history analysis of concrete dams, taking into account the various forms of nonlinearity in the realistic system [16]. In 2008, Arabshahi and Lotfi

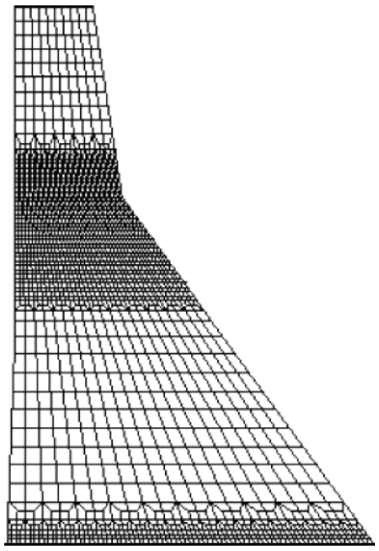

Figure 19: Finite element model of Koyna dam for non-linear analysis.

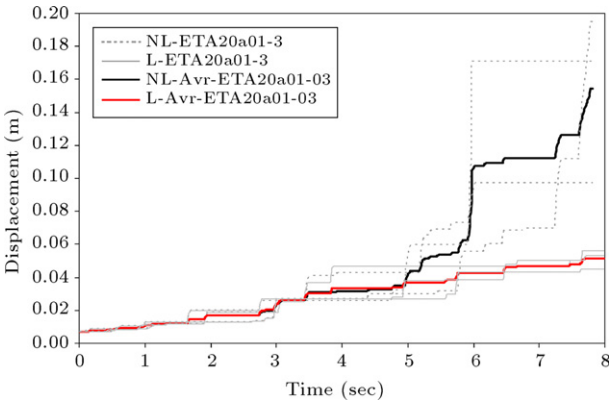

Figure 20: Horizontal displacement at top of Koyna dam under ET acceleration functions.

studied the various possibilities of natural isolation occurring along the dam-foundation interface during an earthquake on the seismic response of an existing gravity dam. Plasticity-based formulation is used in the local stress space of interface elements to model sliding, as well as partial opening, along the dam base [17].

The finite element model of the Koyna dam for non-linear analyses is illustrated in Figure 19. The dam body includes 2266 nodes and 2160 elements, and 1856 nodes are considered for modeling the fluid. For non-linear analysis, an elasto-brittle damping model in which cracked elements do not contribute to the damping matrix is considered for the analysis.

The modulus of elasticity, unit weight and Poisson ratio of the concrete are taken as 30,000 MPa, 2630 kg/m^3 and 0.2, respectively. The tensile and compressive strength of the concrete are taken to be 2.9 and 24.1 MPa, respectively. The fracture energy of concrete considered as 150 N/m and a dynamic magnification factor of 1.2 is considered for the tensile strength and for the fracture energy.

A comparison between the linear and non-linear analysis of the Koyna dam is conducted. As seen in Figure 20, after $t = 5$ s, the results from the linear analysis are not reliable, and nonlinear analysis should be done. In this matter, because in nonlinear analysis the response spectrum method is not

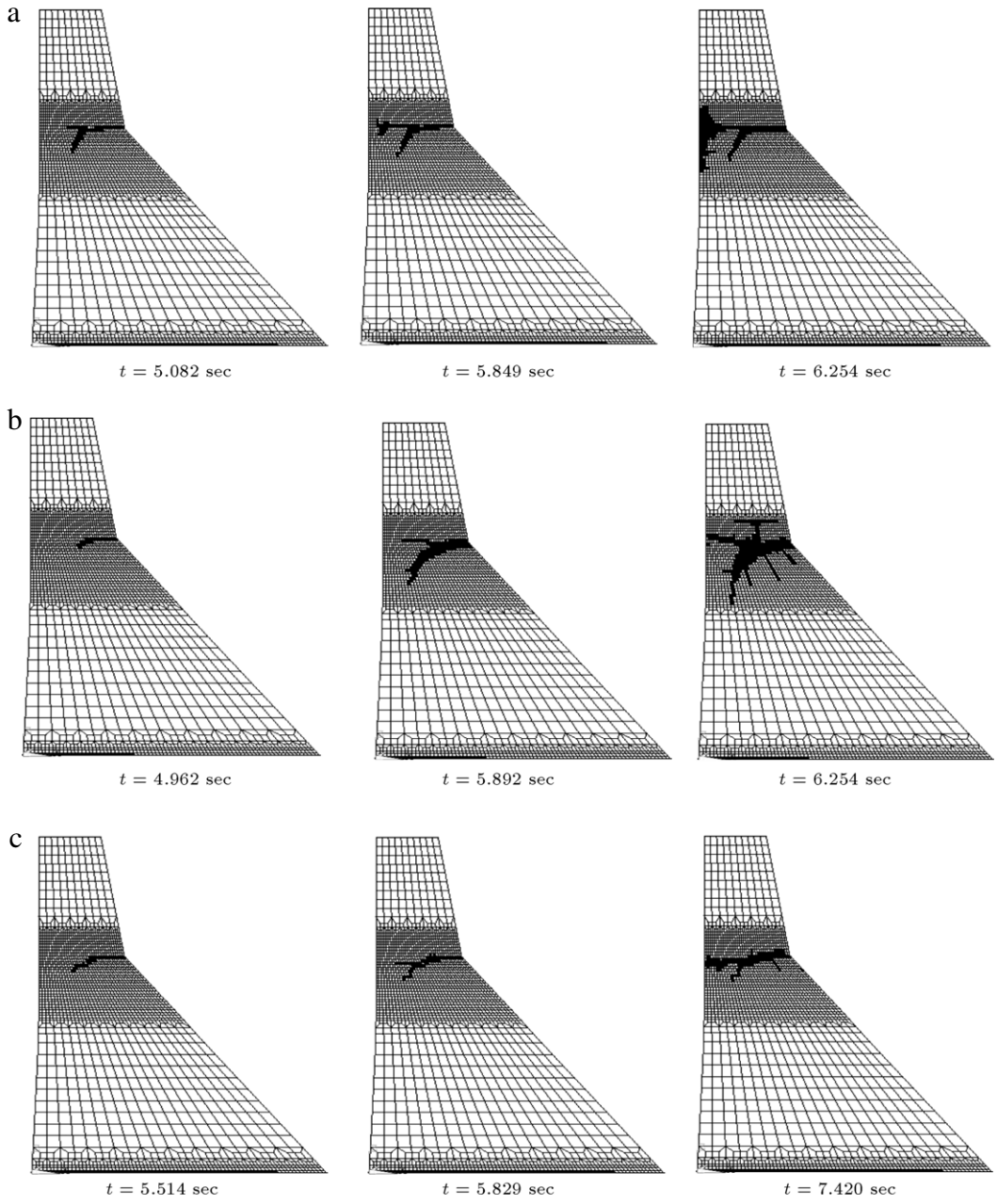

Figure 21: Crack profiles in Koyna dam at different times by ET acceleration function. (a) ETA20a01; (b) ETA20a02; and (c) ETA20a03.

reliable, equivalent time, as discussed in previous sections, is not an appropriate way to predict the nonlinear response of dams. Therefore, the behavior of dam under the Koyna earthquake cannot be predicted reliably by the ET method, by equivalent time, and another method for calibration of ET acceleration functions in nonlinear analysis should be applied (this matter is under investigation). However, the general behavior of the dam and damages can be prognosticated by the ET method, as crack profiles at three different times are evaluated by each ET acceleration function (Figure 21).

It is obvious from Figures 20 and 21 that cracks initiate at a time between 2 s and 3 s, but the behavior of the dam remains almost linear. After $t = 5$ s, cracks develop in the dam body, as shown in the figures, and nonlinear behavior occurs after this time. Crack profiles in these figures are similar to those obtained by previous researchers under the Koyna earthquake [18–20].

As discussed at the end of Section 4, after $t = 5$ s, nonlinear analysis that matches the limit of the linear analysis in this section is necessary.

This paper aims to show application of the ET method in linear analysis and the potential of this method in the nonlinear analysis of concrete dams. However, application of this method in the nonlinear analysis of concrete gravity dams needs more investigation.

7. Conclusion

In this paper, application of the Endurance Time method in linear analysis and the potential of this method in the nonlinear seismic analysis of concrete gravity dams have been investigated. Based on this study, the following conclusions can be drawn:

1. Using the concept of equivalent time, results of linear analysis under real earthquakes can be predicted with reasonable accuracy using the ET method.
2. The critical level of an earthquake in which tensile stress is below allowable stress, can be obtained by the ET method. Comparing this value with the value obtained from a seismic hazard analysis of the site, the safety of a concrete gravity dam can be evaluated.
3. The maximum allowable PGA for seismic design can be obtained using the ET method with reasonable accuracy.
4. The ET method predicted crack profiles in the studied dam during applied earthquakes. However, further investigation is required for extending the application of this method to nonlinear analysis.

Acknowledgments

The authors appreciate the support of this research by the Water Resources Institute under contract No. 59868/152 and also the Research Council and the Structure and Earthquake Engineering Center of Excellence at Sharif University of Technology.

References

[1] Estekanchi, H.E., et al. "Endurance time method for seismic analysis and design of structures", *Scientia Iranica*, 11(4), pp. 361–370 (2004).
[2] Estekanchi, H.E., et al. "Application of endurance time method in linear seismic analysis", *Engineering Structures*, 29(10), pp. 2551–2562 (2007).
[3] Riahi, H.T., et al. "Estimates of average inelastic deformation demands for regular steel frames by the endurance time method", *Scientia Iranica*, 16(5), pp. 388–402 (2009).
[4] Riahi, H.T. and Estekanchi, H.E. "Seismic assessment of steel frames with endurance time method", *J. of Constructional Steel Research*, 66(6), pp. 780–792 (2010).
[5] Valamanesh, V., et al. "Application of endurance time method in seismic analysis and design of concrete gravity dams (in Persian)", *Sharif J. of Science and Technology*, 26(1), pp. 105–118 (2010).
[6] Valamanesh, V., et al. "Characteristics of second generation endurance time acceleration functions", *Scientia Iranica*, 17(1), pp. 53–61 (2010).
[7] Hall, R.L., et al. "Seismic stability evaluation of Folsom dam and reservoir project; report 3, concrete gravity dam", *Technical Report* GL-87-14, US Army Engineer Waterways Experiment Station, Vicksburg, MS 1989.
[8] Raphael, J.M. "Mass concrete properties for seismic evaluation of Engel bright dam, Folsom dam, and pine flat dam", Prepared under Contract No. DACW05-86-P-1049 for the US Army Engineer Distinct, Sacramento 1986.
[9] Chopra, A.K. and Chakabarti, P. "The earthquake experience at Koyna dam and stresses in concrete gravity dams", *Earthq. Eng. Struct. Dyn.*, 1(2), pp. 151–164 (1972).
[10] Ghannat, Y. "Seismic performance and damage criteria for concrete dams", 3rd US-Japan Workshop on Advanced Research on Earthq. Enging. for Dams, San Diego, USA (2002).
[11] Skrikerud, P.E. and Bachmann, H. "Discrete crack modeling for dynamically loaded unreinforced concrete structures", *Earthq. Eng. Struct. Dyn.*, 14(2), pp. 297–315 (1986).
[12] Lee, J., et al. "A joint element based on a homogenization technique", *Numerical Models in Geomechanics*, pp. 249–258 (1992).
[13] Vargas-Loli, L. and Fenves, G.L. "Effects of concrete cracking on the earthquake response of gravity dams", *Earthq. Eng. Struct. Dyn.*, 18(4), pp. 575–592 (1989).
[14] Ghaemian, M. and Ghobarah, A. "Staggered solution schemes for dam-reservoir interaction", *J. of Fluids and Structures*, 12(7), pp. 933–948 (1998).
[15] Bhattacharjee, S.S. and Leger, P. "Application of NLFM models to predict cracking in concrete gravity dams", *J. Struct. Eng. ASCE*, 120(4), pp. 1255–1271 (1994).
[16] Asteris, P.G. and Tzamtzis, A.D. "Nonlinear seismic response analysis of realistic gravity dam-reservoir systems", *Int. J. Nonlinear Sciences and Numerical Simulation*, 4(4), pp. 329–338 (2003).
[17] Arabshahi, H. and Lotfi, V. "Earthquake response of concrete gravity dams including dam-foundation interface nonlinearities", *Engineering Structures*, 30(11), pp. 3065–3073 (2008).
[18] Lee, J. and Fenves, G.L. "A plastic-damage concrete model for earthquake analysis of concrete dams", *Earthq. Eng. Struct. Dyn.*, 27(9), pp. 937–956 (1998).
[19] Calayir, Y. and Karaton, M. "A continuum damage concrete model for earthquake analysis of concrete gravity dam-reservoir systems", *Soil Dyn. Earthquake Eng.*, 25(11), pp. 857–869 (2005).
[20] Calayir, Y. and Karaton, M. "Seismic fracture analysis of concrete gravity dams including dam-reservoir interaction", *Comput. Struct.*, 83(19), pp. 1595–1606 (2005).

Vahid Valamanesh received his M.S. degree in Structural Engineering from Sharif University of Technology, Tehran, Iran in 2005. He is currently a Researcher in the Building and Housing Research Center (BHRC), Tehran, Iran. His areas of research include: Structural Dynamics and Earthquake Engineering, as well as Vulnerability Assessments of Structures under Seismic Loading.

Homayoon Estekanchi is Associate Professor of Civil Engineering at Sharif University of Technology (SUT). He received his Ph.D. in Civil Engineering from SUT in 1997 and has been a Faculty Member at SUT since that time. He is a member of the Iranian Construction Engineers Organization, ASCE, Iranian Inventors Association and several other professional associations. His research interests include a broad area of topics in Structural and Earthquake Engineering, with a special focus on the Design of Tall Buildings and Industrial Structures.

Abolhassan Vafai, Ph.D., is a Professor of Civil Engineering at Sharif University of Technology. He has authored/co-authored numerous papers in different fields of Engineering: Applied Mechanics, Biomechanics, Structural Engineering (steel, concrete, timber and offshore structures). He has also been active in the area of higher education and has delivered lectures and published papers on challenges of higher education, the future of science and technology and human resources development.

Mohsen Ghaemian is an associate professor at Sharif University of Technology. His research interest is mostly on nonlinear dynamic analysis of concrete dams.